Influence of Surface Composition and Pore Structure on Cr(III) Adsorption onto Activated Carbons

T. Cordero and J. Rodriguez-Mirasol

Department of Chemical Engineering, University of Malaga, Malaga, Spain

N. Tancredi, J. Piriz, and G. Vivo

Department of Surface Physicochemistry, University of La Republica, Montevideo, Uruguay

J. J. Rodriguez*

Chemical Engineering, University Autonoma of Madrid, 28049 Madrid, Spain

The adsorption of chromium(III) ions from aqueous solutions onto activated carbons prepared from air and CO_2 activation of Eucalyptus sawdust is studied. HNO_3 oxidation of these carbons greatly enhances their ability to retain Cr(III) mainly because of a significant increase of the concentration of carbon−oxygen surface groups. To characterize these surface groups, X-ray photoelectron spectroscopy and temperature-programmed desorption (TPD) were used. The influence of these carbon−oxygen surface groups on chromium adsorption is examined. Upon addition of acidic groups, some other functions of nonacidic character evolving as CO upon TPD seem to contribute to Cr(III) uptake. Modifications of the porous structure upon oxidation and chromium adsorption are investigated. Adsorption into the micropores appears to take place to a significant extent although oxidation of the active carbons leads to a narrowing of the average micropore widths.

Introduction

Activated carbons are the most important commercial adsorbents. One of the fields where they have found more extended applications has been water and wastewater treatment. Although those applications deal most commonly with the removal of organic pollutants, in the last 2 decades the use of activated carbons has gained increasing attention for heavy-metal uptake from aqueous effluents.[1−4] Heavy metals are recognized as highly toxic pollutants, and thus the environmental regulations establish severe restrictions in terms of concentration limits in the effluents. This demands the use of high-efficiency techniques, and in that context adsorption has been claimed as one alternative solution capable of competing in some circumstances with the most widely used alkaline precipitation.

Chromium is one of the most studied heavy metals because of its relative frequency and high toxicity. It is present commonly as Cr(VI) and Cr(III). Although the first is the most hazardous chromium species, the second requires also particular attention, and the scientific and technical literature reports many studies on Cr(III) removal from industrial wastewaters. Tanneries are one of the most representative industries with regard to Cr(III) pollution. This industry represents an important contribution to the Uruguayan economy as well as in many other countries or regions, and thus there is a need for cost-effective treatment systems to control the presence of this pollutant in the aqueous offstreams from that industrial sector. In this respect, adsorption may be a feasible way of competing with the most established alkaline precipitation provided that low-cost activated carbons could be used as adsorbents. In previous studies we have reported the preparation of activated carbons from Uruguayan Eucalyptus sawdust.[5,6] Some of us have reported recently our results on Cr(III) adsorption with those carbons.[7] In the present paper we analyze the factors determining the capacity of the activated carbons to retain Cr(III) from aqueous solutions.

Work on Cr(III) adsorption with activated carbons has been reported in the literature.[8−14] As a general conclusion, the presence of oxygen surface groups has been pointed out as a main factor affecting Cr(III) adsorption. The influence of pH and the porous structure of the carbons have also been studied. Despite these valuable contributions, there is still room to learn more about the influence of the surface chemistry and porous structure of the activated carbons on Cr(III) adsorption, and this work intends to be a contribution in that respect. To perform our study, we have prepared different activated carbons by CO_2 and air activation of a Eucalyptus char as well as from further HNO_3 oxidation of those carbons. The surface chemical composition of the carbons has been studied by X-ray photoelectron spectroscopy (XPS) and temperature-programmed desorption (TPD), and their porous structure has been characterized before and after chromium adsorption. The corresponding heat-treated carbons have also been studied.

Experimental Section

The activated carbons used in this work were prepared from a char resulting from carbonization of *Eucalyptus grandis* sawdust at 800 °C in a N_2 atmosphere. Two activated carbons were prepared by CO_2 (D) and air (A) partial gasification of that char at 800

* To whom correspondence should be addressed. E-mail: juanjo.rodríguez@uam.es.

10.1021/ie020210f CCC: $22.00
Published on Web 10/19/2002

Table 1. Elemental Analysis of the Carbons (% Dry Basis Including Ash Content)

carbon sample	nomenclature	C (%)	H (%)	N (%)	O (%)
char	C800	90.30	2.10	0.16	6.20
CO_2-activated	D	92.95	0.69	0.16	6.20
air-activated	A	84.16	0.93	0.18	14.73
HNO_3-oxidized D	OD	72.00	1.07	0.72	26.21
HNO_3-oxidized A	OA	67.51	1.18	0.83	30.48
TPD carbon from D	DH	93.05	0.42	0.14	6.39
TPD carbon from A	AH	92.57	0.55	0.15	6.73
TPD carbon from OD	ODH	93.89	0.43	0.92	4.76
TPD carbon from OA	OAH	91.83	0.58	1.21	6.38

and 400 °C, respectively. The carbonization and gasification runs were carried out in a horizontal tube furnace under continuos gas flow. Details on the experimental system and operating conditions can be consulted elsewhere.[5,6] These carbons were treated with a concentrated HNO_3 aqueous solution (70% by weight) at 80 °C to obtain the corresponding oxidized carbons (OD and OA, respectively).

High-temperature treatment was performed with the original and oxidized active carbons by TPD experiments under a continuous He flow at a 10 °C/min heating rate up to a final temperature of 900 °C (H series carbons). The evolution of CO and CO_2 was analyzed by mass specrometry (MS), using a MSC 200 model Balzers apparatus with a tungsten filament.

The surface of all of the carbons, including that resulting from TPD, was analyzed by XPS in a 5700 model Physical Electronics equipment using Mg Kα (1253 eV) radiation. These analyses were carried out as well for the chromium-adsorbed carbons.

The porous structure of the carbons before and after chromium adsorption was characterized from N_2 (77 K) and CO_2 (273 K) adsorption using a Quantachrome Autosorb-1 apparatus. The Brunauer−Emmett−Teller (BET), DR, and t methods were used to determine the values of the apparent surface area, micropore volumes, and external or nonmicroporous surface, respectively.[15,16] The Halsey equation was used for the t method.

Adsorption of Cr(III) was accomplished at 30 °C in 150 mL stoppered bottles placed in a thermostated SBS30 Stuart Scientific shaker. A volume of 100 mL of a $Cr(NO_3)_3{\cdot}9H_2O$ solution was used in all of the experiments by varying the initial Cr(III) to carbon ratio in order to obtain the corresponding adsorption isotherms. The pH of all of these solutions was measured before and after adsorption, and it always remained in the vicinity of 3−3.5. The equilibrium Cr(III) concentrations were obtained from atomic absorption in a 475ABD model Varian apparatus.

The identification of all of the carbons together with their elemental composition is given in Table 1. Elemental analyses were obtained with a 2400 C Perkin-Elmer apparatus.

Results and Discussion

Table 2 reports the Cr(III) monolayer Langmuir adsorption capacities obtained for the original and oxidized carbons from the 25 °C adsorption isotherms. The table includes also the surface covered by Cr(III) taking a molecular diameter of 0.922 nm for hexahydrated trivalent chromium,[17] which is the dominant species within the pH range used in our experiments.[13,18] As can be clearly seen, a considerable

Table 2. Cr(III) Langmuir Adsorption Capacities of the Activated Carbons

active carbon	adsorption capacity (mg of Cr(III)/ g of activated C)	surface area covered by Cr(III) (m^2/g)
A	0.8	6
D	0.4	3
OA	31.5	242
OD	26.3	202

increase of Cr(III) adsorption occurs upon carbon oxidation. This is in agreement with the results reported by other authors,[11,14] although in the case of our carbons the differences become even more pronounced. The air-activated carbon (A) shows twice more adsorption capacity than the CO_2-activated one (D), although in both cases adsorption remains fairly poor before oxidation of the carbons. Cr(III) uptake of the carbons vary clearly with their oxygen contents (Table 1) because of the oxygen surface complexes, which may act as specific sites to Cr(III) adsorption.

To learn about the chemical composition of the surface of these carbons, we obtained XPS spectra of the original and oxidized carbons in the C(1s), O(1s), N(1s), and Cr(2p) spectral regions. Figure 1 presents the C(1s) XPS spectrum of the OD carbon, which shows an asymmetric tailing that indicates a contribution of oxygen-containing functional groups.[19−21] This spectrum has been deconvoluted in four symmetric peaks of the Gaussian type. In addition to a main peak at 284.5 eV due to graphitic carbon, the spectrum can be fitted to three peaks centered at 285.9, 288.3, and 290.7 eV that can be associated with C−O bonds of functional groups such as hydroxyl and/or ethers, with a C═O bond as in the carbonyl group, and with a −COO− bond characteristic of carboxylic and/or ester groups, respectively.[22] The O(1s) XPS spectrum for OD carbon (Figure 2) was fitted to three peaks with binding energies of 531.7, 533.5, and 535.8 eV that have been assigned to the O═C bond, to the C−O and/or HO−C bonds, and to adsorbed water, respectively.[22] High-temperature treatment of this carbon leads to a significant reduction of the intensity of these three peaks, indicating a substantial loss of surface oxygen. Similar results were obtained for the A series carbons. The oxidized carbons showed also a band centered at 405.8 eV in the N(1s) region associated with nitro groups resulting from HNO_3 oxidation. At lower binding energy values (398−402 eV), a wide band of low intensity was observed which may be assigned to N bonded to basal C.[22,23] This band remains after TPD.

Table 3 shows the surface atomic concentration for C, O, and N of the different carbons studied, calculated from the corresponding peak areas of XPS divided by the appropriate sensitivity factors.[24] The results of this table show that partial gasification with CO_2 and with air produces an increase of the amount of oxygen on the surface of the carbon, but air oxidation introduces more oxygen surface complexes than the CO_2 one, for the same burnoff level (50%). Nitric acid oxidation increases the amount of surface oxygen by 188% for D carbon and only by 68% for A carbon. Despite this result, the total amount of surface (Table 3) and bulk (Table 1) oxygen added to C800 by both activation and oxidation treatments is slightly higher for OA carbon. This can be clearly observed by calculation of the O/C atomic ratio.

The O/C surface atomic ratios of the carbons as obtained from XPS are given in Table 4. For the sake of comparison, we have included the corresponding bulk

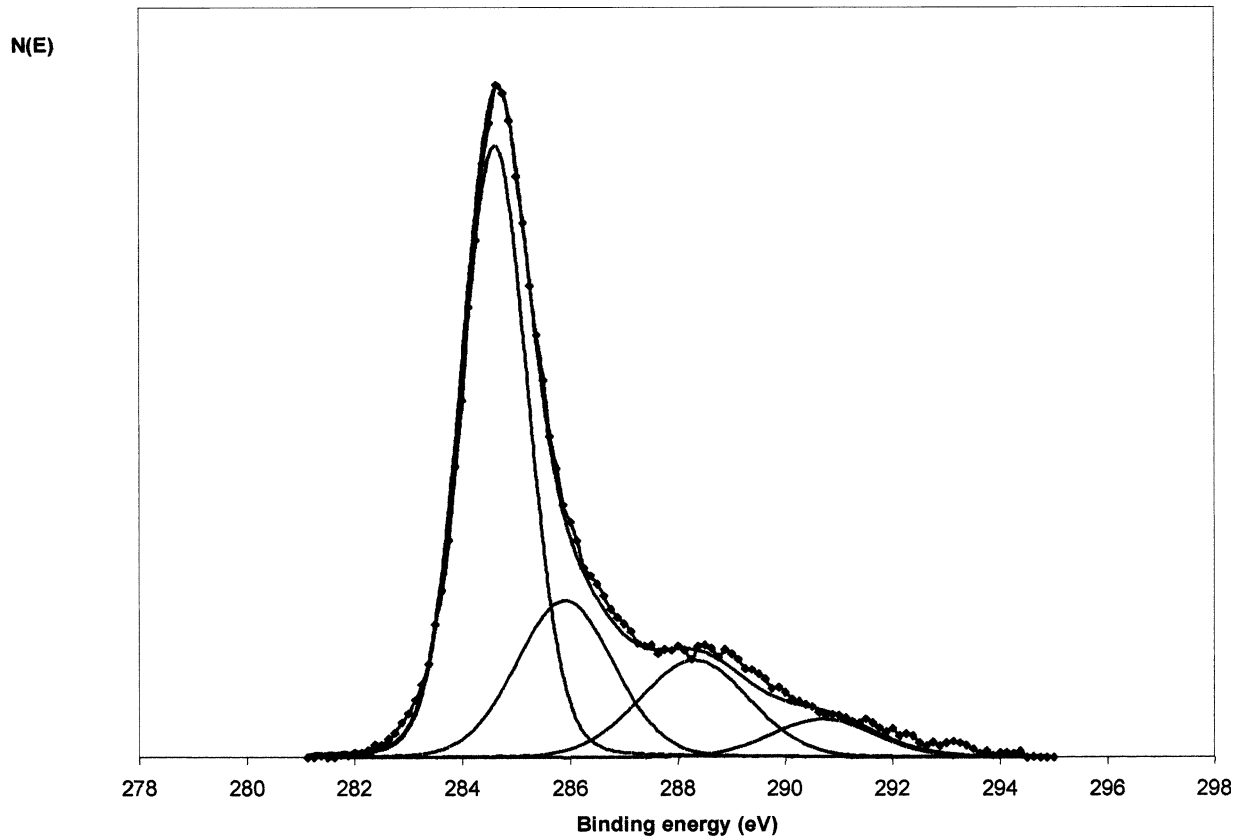

Figure 1. Deconvolution of the C(1s) region XPS spectrum corresponding to OD carbon.

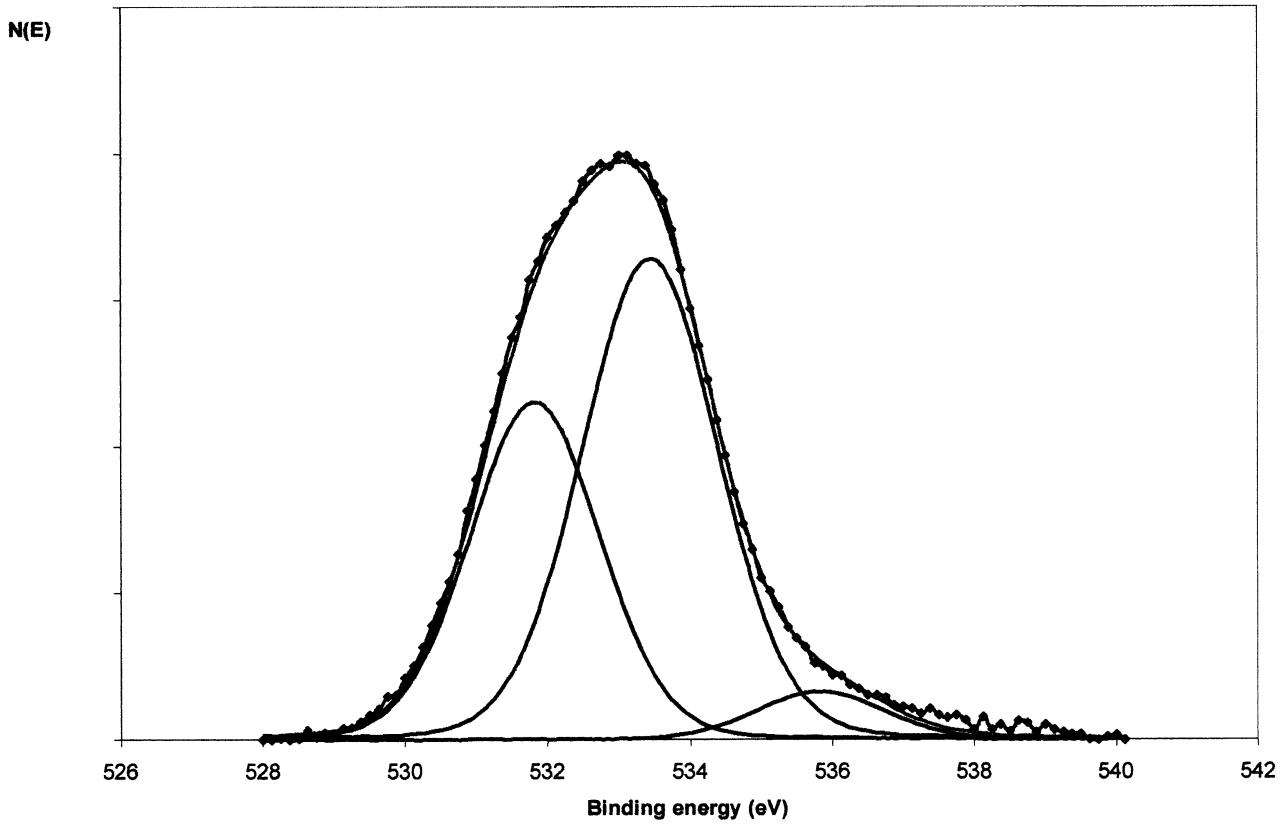

Figure 2. Deconvolution of the O(1s) region XPS spectrum corresponding to OD carbon.

values of the O/C ratio derived from elemental analyses. In the case of oxidized carbons, the bulk ratio is higher than the surface ratio (by 23% in the case of A carbon), suggesting that some of the surface oxygen groups are located deep into the micropores. These oxygen groups would be more difficult to remove upon TPD, with this being consistent with the somewhat lower values obtained for the surface O/C ratio with regard to the

Table 3. Surface Atomic Concentration Obtained from the C(1s), O(1s), and N(1s) XPS Regions for the Different Carbons Studied

carbon sample	C(1s)	O(1s)	N(1s)
C800	95.28	4.72	
D	93.32	6.68	
A	87.12	12.61	0.27
OD	79.66	19.26	1.08
OA	77.37	21.22	1.41
DH	96.24	3.76	
AH	95.11	4.89	
ODH	95.79	3.49	0.72
OAH	95.20	3.74	1.06

Table 4. O/C Atomic Ratios of the Active Carbons

carbon	surface ratio ($\times 10^2$)	bulk ratio ($\times 10^2$)
D	7.1	5.0
A	14.5	13.1
OD	24.2	27.3
OA	27.4	33.8
DH	3.9	5.0
AH	5.1	5.5
ODH	3.7	3.8
OAH	3.9	5.2

Table 5. Surface Atomic Concentration Obtained by Deconvolution of C(1s) and O(1s) XPS Regions for the Carbons of the D Series

		surface atomic concn (%)			
peak	assignation	D	DH	OD	ODH
C(1s)					
284.5	C−C	66.4	68.15	53.15	64.45
285.9	C−O; C−O−C; C−OH	13.33	16.33	11.96	19.68
288.3	C═O	7.63	7.49	8.46	7.44
290.7	−COO−	5.96	4.26	6.09	4.22
O(1s)					
531.7	O═C	1.25	2.60	7.52	1.52
533.5	O−C; HO−C	5.43	1.16	11.74	1.97
535.8	adsorbed water			1.08	0.72

corresponding bulk ones in the case of the thermally treated carbons (H carbons).

Table 5 presents the surface atomic concentration of different carbon−oxygen groups, calculated from the deconvolution of the XPS peaks, for the carbons of the D series. These results confirmed that oxidation leads to a significant increase of the C−O to C−C ratio, which rises from 0.5 in carbon D to 0.88 in OD. Nevertheless, the acidic C−O to total C−O atomic ratio remains fairly constant (0.22 in carbon D and 0.23 in OD). Similar results were obtained for the carbons of the A series.

XPS spectra of the carbons with adsorbed chromium were also obtained. The Cr(2p) spectrum for OA carbon (Figure 3) showed a main band centered at 576.8 eV accompanied by a secondary one displaced 9.8 eV to higher binding energy (586.6 eV), with an area ratio of 1:0.5, which correspond to the characteristic values of Cr(III). No evidence of oxidation of Cr(III) to Cr(VI) was observed onto the carbons surface. This behavior was observed in all of the Cr(III) adsorbed carbons. With regard to the C(1s) and O(1s) regions, no significant shifts in the binding energy were detected with respect to the corresponding carbons before Cr(III) adsorption, indicating that there is no formation of bonds between the Cr(III) ions and the oxygen surface groups.

TPD provides information on the nature of the carbon−oxygen groups. Those carboxylic acids and lactone groups evolve as CO_2 upon heating, and carboxylic anhydride produce both $CO_2 + CO$, whereas CO derives from phenols, ethers, and carbonyls/quinones

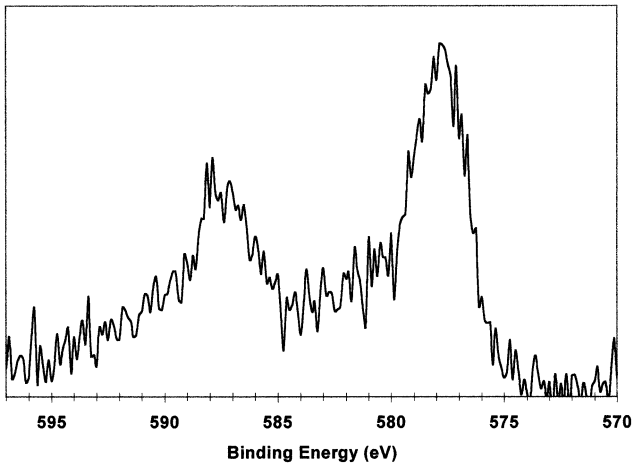

Figure 3. Cr(2p) XPS of the chromium-adsorbed OA carbon.

groups.[25−32] Figures 4 and 5 show the TPD curves obtained for the original and oxidized active carbons.

The air-activated carbon and its oxidized form release more CO and CO_2 than the corresponding CO_2-activated carbons, indicating that significantly more oxygen complexes are formed during partial gasification in air than in CO_2.[33] TPD of carbon D, prepared by partial gasification with CO_2, yields predominantly CO, which is evolved at higher temperatures than in the case of carbon A, suggesting that more stable C−O surface complexes are formed by partial gasification in CO_2.[19] The TPD of carbon A shows that CO_2 is evolved at relatively high temperature. Hall and Calo[34] suggested that the secondary reaction between CO and oxygen surface complexes may be responsible for the release of CO_2 at higher temperatures. However, the relatively low heating rate used in our TPD experiments (5 °C/min) leads to a very low concentration of CO in the pores, which prevents significant occurrence of secondary reactions.[33] Thus, the results of the TPD experiments carried out in this study can be considered to be representative of the original state of the C−O complexes of the surface of the carbons. Nevertheless, for all of the carbons, the amount of CO evolved exceeds considerably that of CO_2, even in the case of oxidized carbons (724 μmol of CO versus 130 μmol of CO_2/g of carbon for the case of OA carbon), suggesting that most of the carbon−oxygen groups present in these carbons are of nonacidic nature. Nevertheless, phenolic hydroxyl groups, which react as weakly acidic and evolve as CO, may also be present to some extent. This result differs from that reported by Aggarwal et al. for other types of HNO_3 oxidized active carbons.[14] Those active carbons showed more comparable Cr(III) uptakes than ours. Thus, according to ours results, also some of the carbon−oxygen groups evolving CO upon TPD must contribute to the Cr(III) adsorption capacity, probably those forming hydroxyl groups.

To learn about the influence of the porous structure of the active carbons on Cr(III) adsorption, we measured the N_2 (77 K) and CO_2 (273 K) adsorption isotherms of the original and oxidized as well as of the heat-treated carbons. Figure 6 shows the N_2 isotherms of the A series. All of the isotherms correspond to essentially microporous solids as revealed by the steep uptake at low relative pressure, although the slope of the nearly horizontal branch indicates some contribution of mesoporosity. The carbons of the A series show lower adsorption values than the corresponding D samples,

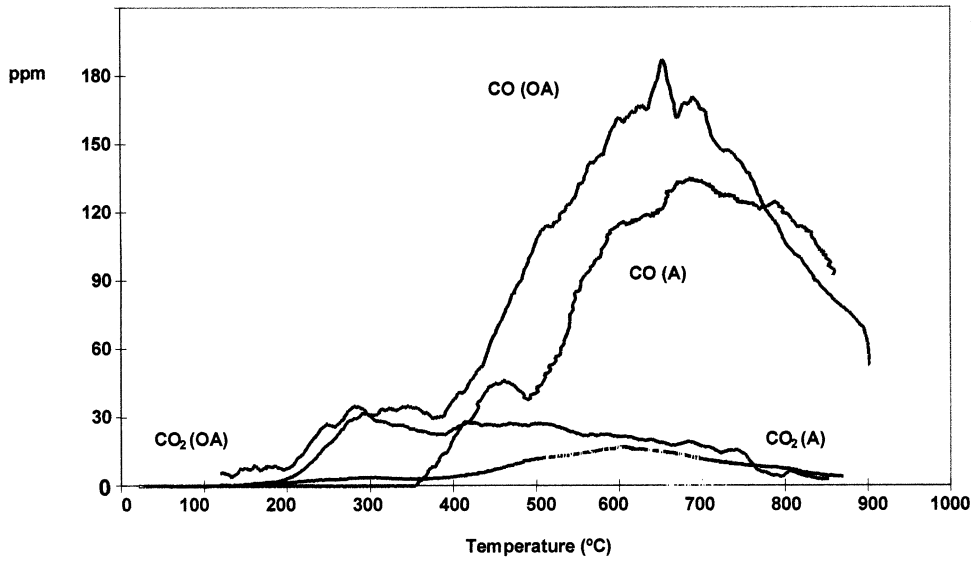

Figure 4. TPD curves for the A and OA carbons.

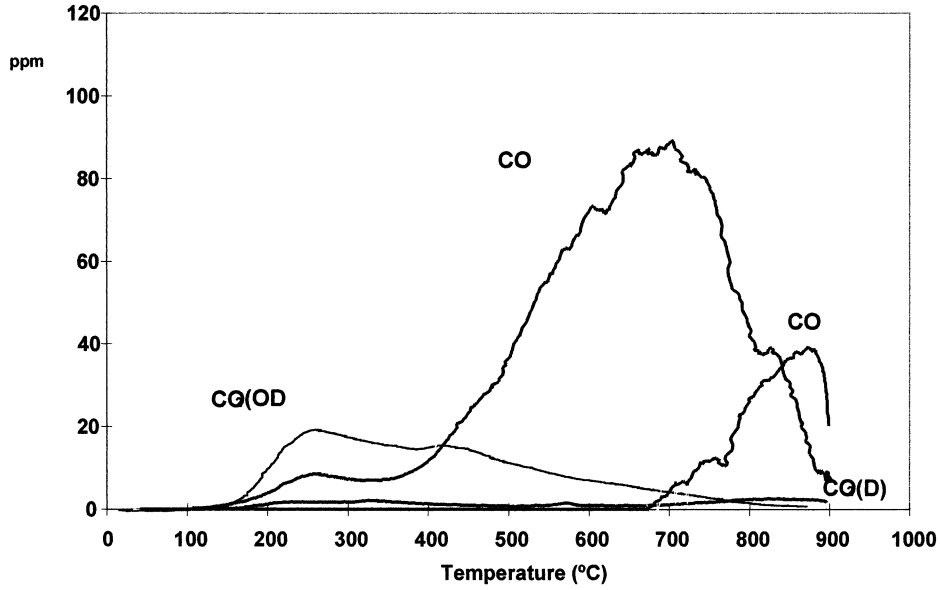

Figure 5. TPD curves for the D and OD carbons.

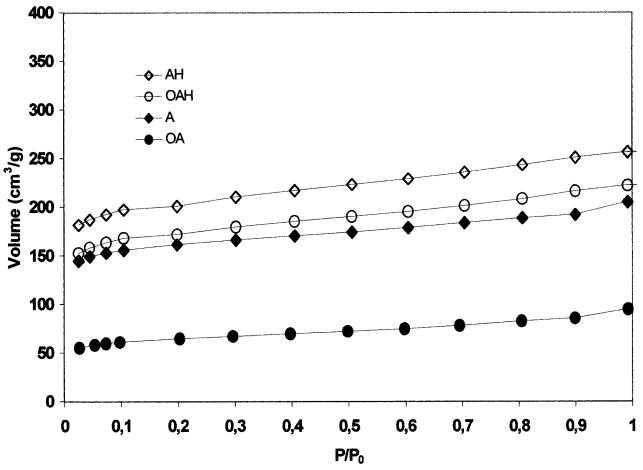

Figure 6. N_2 adsorption isotherms of the active carbons of the A series.

and in both series the isotherms of the oxidized carbons fall well below those of the original ones. This is more pronounced in the case of the air-activated carbon (A). The heat treatment accompanying TPD of the carbons leads to an increase of the N_2 adsorption capacity. These variations on the N_2 adsorption values are correlated to the relative amount of surface oxygen groups of these carbons. Thus, the presence of these groups on the walls of the micropores may reduce significantly the pore volume available for N_2 uptake, and even blockage of pore entrances may take place to some extent, particularly in the case of the OA carbon, where the decrease of N_2 adsorption is more pronounced.

Table 6 reports the values of the BET surface area and micropore volumes of the carbons, the last ones as determined from both the t method (V_t) and the DR equation (V_{DR}) applied to the N_2 and to the CO_2 isotherms, respectively. Comparison of those two values provides information on the relative distribution of the micropore size. The external or nonmicroporous surface of the carbons (S_{ext}) obtained from the t method is also included.

In both the A and D carbons, the values of the BET surface area and micropore volume decrease upon oxidation, inversely to what happened with chromium

Table 6. Characterization of the Porous Structures of the Active Carbons

carbon	A_{BET} (m^2/g)	$V_t(N_2)$ (cm^3/g)	$V_{DR}(CO_2)$ (cm^3/g)	S_{ext} (m^2/g)
D	890	0.41	0.37	206
A	600	0.26	0.27	126
OD	730	0.34	0.31	183
OA	240	0.11	0.17	145
DH	870	0.41	0.37	216
AH	790	0.36	0.28	197
ODH	1060	0.49	0.31	278
OAH	680	0.29	0.18	174

Table 7. Characterization of the Porous Structures of the Oxidized Active Carbons after Chromium Adsorption

carbon	A_{BET} (m^2/g)	$V_t(N_2)$ (cm^3/g)	$V_{DR}(CO_2)$ (cm^3/g)
CrOD	530	0.25	0.28
CrOA	110	0.06	0.14

adsorption capacity. This is particularly noticeable in the case of the air-activated carbon. The OA carbon, which showed the higher chromium uptake, is by far the poorer one in terms of porosity, with a fairly low apparent surface area and micropore volume. Thus, it appears that none of those two structural characteristics are determining factors for Cr(III) adsorption, this being essentially determined by the presence of carbon−oxygen groups on the surface of the carbons.

The micropores of the original and oxidized carbons fall mostly within the narrow size range (about one to two N_2 molecular diameters, namely, 0.3−0.7 nm) as suggested by the closeness of the V_t and V_{DR} values. Oxidation leads to a narrowing of the microporous structure. In the case of the OA carbon, the DR micropore volume obtained from CO_2 adsorption is even appreciably larger than the total micropore volume represented by the V_t value. This indicates fairly narrow micropores, which was confirmed by the micropore size distributions obtained by the MP method. The heat-treated carbons after TPD show substantially larger differences between the V_t and V_{DR} values indicative of a widening of the microporosity which can be explained as a result of desorption of carbon−oxygen groups from micropore walls.

The N_2 and CO_2 adsorption isotherms of the chromium-adsorbed active carbons have also been obtained. Characterization of their porous structures is reported in Table 7. As can be seen, the BET surface area and the micropore volume accessible to N_2 (V_t) undergo a significant decrease upon Cr(III) adsorption (see the corresponding values for OA and OD in Table 6). Comparison of the V_t and V_{DR} values reveals the presence of narrow micropores in the carbons after chromium adsorption which is more pronounced in the OA carbon, the one with a higher chromium adsorption capacity.

It has been reported in the literature[35] that the strong electrostatic interactions of the positive charge ions with the negatively charged surface of the carbon may produce the adsorption of cations as Cr(III) on the micropore entrance, which would explain the decrease in the BET surface area and micropore volume upon Cr(III) adsorption. However, it has to be pointed out that the external surface area of the oxidized carbons falls below the area covered by the adsorbed chromium as calculated from the Langmuir capacity (see Table 2), suggesting a contribution of micropores to Cr(III) uptake. Moreover, assuming that chromium adsorption takes place essentially on carbon−oxygen surface groups, it has to be considered that the relative atomic concentration of oxygen on the surface of those carbons is no more than 25−30%. Besides, the Cr/O atomic ratio as obtained from XPS of the oxidized carbons after chromium adsorption was lower than 0.05 in the case of OA and below 0.04 for OD. Thus, even when the substantially higher cross-sectional area of the chromium ions relative to that of oxygen atoms is considered, there is still a large difference between the calculated area covered by chromium and the external surface area available for Cr(III) adsorption. This suggests that chromium uptake into the micropores of these carbons must be of some relative importance.

The narrow microporosity of the oxidized carbons may hinder the entrance of Cr(III), at least in the form of hexaquo ions. Then, the access of chromium into the micropores must be accompanied by some kind of transformation which reduces the critical dimension of the resulting species. Jayson et al.[10] working with microporous activated charcoal cloths have suggested a two-stage process consisting of a primary adsorption followed by dehydration of adsorbed chromium ions which would migrate into the micropores. Besides, according to the speciation diagram for Cr(III) in an aqueous solution,[13] at pH 3 Cr^{3+} and $Cr(OH)^{2+}$ species are present in an approximate distribution of 60 and 40%, respectively. $Cr(OH)^{2+}$ ion presents a lower size and charge than the Cr(III) in the form of hexaquo ion, which would permit an easier adsorption into the narrow micropores of the oxidized carbons.

Conclusion

Activated carbons produced from Eucalyptus sawdust by partial gasification with air or CO_2 show a reasonably good adsorption capacity for Cr(III) adsorption after HNO_3 oxidation. This treatment leads to a significant increase of carbon−oxygen groups on the surface of the carbons, which is the determining factor enhancing Cr(III) uptake. In addition to acidic groups, other carbon−oxygen groups of nonacidic character as well as phenolic groups, which evolve as CO upon TPD, must have a significant relative contribution to chromium adsorption.

The external surface of the carbons available for chromium adsorption appears to be rather insufficient to account for the observed Cr(III) uptake, and a significant relative amount of it must be retained in the micropores even though the oxidized carbons show a predominantly narrow microporous structure. Thus, the access of trivalent chromium into the micropores may not be in the form of hexaquo ion.

Acknowledgment

This research has been possible in part because of the financial support received by N. Tancredi from CSIC-Universidad de La República (Uruguay) to cover a stay at the Chemical Engineering Department of the University of Malaga.

Literature Cited

(1) Ferro-García, M. A.; Rivera-Utrilla, J.; Bautista-Toledo, I. Removal of Lead from Water by Activated Carbons. *Carbon* **1990**, *28* (4), 545.

(2) Marzal, P.; Seco, A.; Gabaldón, C.; Ferrer, J. Cadmium and Zinc Adsorption onto Activated Carbon: Influence of Temperature, pH and Metal/Carbon Ratio. *J. Chem. Technol. Biotechnol*. **1996**, *66*, 279.

(3) Seco, A.; Marzal, P.; Gabaldón, C.; Ferrer, J. Adsorption of Heavy Metals from Aqueous Solutions onto Activated Carbon in Single Cu and Ni Systems and in Binary Cu−Ni, Cu−Cd and Cu−Zn Systems. *J. Chem. Technol. Biotechnol*. **1997**, *68*, 23.

(4) Namasivayam, C.; Kadirvelu, K. Uptake of Mercury (II) from Wastewater by Activated Carbon from an Unwanted Agricultural Solid By-product: Coirpith. *Carbon* **1999**, *37*, 79.

(5) Tancredi, N.; Cordero, T.; Rodríguez-Mirasol, J.; Rodríguez, J. J. Activated carbons from Uruguayan eucalyptus wood. *Fuel* **1996**, *75*, 1701.

(6) Tancredi, N.; Cordero, T.; Rodríguez-Mirasol, J.; Rodríguez, J. J. Activated carbons from Eucalyptus wood. Influence of the carbonization temperature. *Sep. Sci. Technol.* **1997**, *32*, 1115.

(7) Milich, P.; Möller, F.; Píriz, J.; Vivó, G.; Tancredi, N. Influence of surface properties of activated carbons on Cr(III) adsorption from aqueous water solutions. *Sep. Sci. Technol.* **2002**, in press.

(8) Huang, C. P.; Wu, M. H. Chromium removal by carbon adsorption. *J. Water Pollut. Control Fed*. **1975**, *47*, 2437.

(9) Huang, C. P.; Wu, M. H. The removal of chromium(VI) from dilute aqueous solution by activated carbon. *Water Res*. **1977**, *11*, 673.

(10) Jayson, G. G.; Sangster, J. A.; Thompson, G.; Wilkinson, M. C. Adsorption of Chromium from Aqueous Solution onto Activated Charcoal Cloth. *Carbon* **1993**, *31*, 487.

(11) Bautista-Toledo, I.; Rivera-Utrilla, J.; Ferro-García, M. A.; Moreno-Castilla, C. Influence of the Oxygen Surface Complexes of Activated Carbons on the Adsorption of Chromium Ions from Aqueous Solutions: Effect of Sodium Chloride and Humic Acid. *Carbon* **1994**, *32*, 93.

(12) Moreno-Castilla, C.; Ferro-García, M. A.; Rivera-Utrilla, J.; Joly, J. P. A TPD Study of Chromium Catalysts Suported on an Oxidized and Nonoxidized Activated Carbon. *Energy Fuels* **1994**, *8*, 1233.

(13) Leyva-Ramos, R.; Fuentes-Rubio, L.; Guerrero-Coronado, R. M.; Mendoza-Barron, J. Adsorption of trivalent chromium from aqueous solutions onto activated carbon. *J. Chem. Technol. Biotechnol*. **1995**, *62*, 64.

(14) Aggarwal, D.; Goyal, M.; Bansal, R. C. Adsorption of Chromium by Activated Carbon from Aqueous Solution. *Carbon* **1999**, *37*, 1989.

(15) Gregg, S. J.; Sing, K. S. *Adsorption, Surface Area and Porosity*; Academic Press: London, 1982.

(16) Lowell, S.; Shields, J. E. *Powder surface area and porosity*; Chapman and Hall: New York, 1987.

(17) Nightingale, E. R. Phenomenological theory of ion solvation. Effective radii of hydrated ions. *J. Phys. Chem*. **1959**, *63*, 1381.

(18) Rai, D.; Sass, B. M.; Moore, D. A. Chromium(III) hydrolysis constants and solubility of chromium(III) hydroxide. *Inorg. Chem*. **1987**, *26*, 345.

(19) Kelemen, S. R.; Freund, H. XPS Characterization of Glassy-Carbon Surfaces Oxidized by O_2, CO_2 and HNO_3. *Energy Fuels* **1988**, *2*, 111.

(20) Gardner, S. D.; Singamsetty, C. S. K.; Booth, G. L.; He, G. Surface Characterization of Carbon Fibers using Angle-Resolved XPS and ISS. *Carbon* **1995**, *33* (5), 587.

(21) Park, S. H.; McClain, S.; Tian, Z. R.; Suib, S. L.; Karwacki, C. Surface and Bulk Measurements of Metals Deposited on Activated Carbon. *Chem. Mater*. **1997**, *9*, 176.

(22) Darmstadt, H.; Roy, C.; Kaliagune, S. ESCA Characterization of Commercial Carbon Blacks and of Carbon Blacks from Vacuum Pyrolysis of Used Tyres. *Carbon* **1994**, *32*, 1399.

(23) Wòjtowicz, M. A.; Pels, J. R.; Moulijn, J. A. The fate of nitrogen functionalities in coal during pyrolysis and combustion. *Fuel* **1995**, *74*, 507.

(24) Ikeo, N.; Iijima, Y.; Niimura, N.; Sigematsu, M.; Tazawa, T.; Matsumoto, S.; Kojima, K.; Nagsawa, Y. *Handbook of X-ray Photoelectron Spectroscopy*; JEOL: Cranford, NJ, 1991.

(25) Figueiredo, J. L.; Pereira, M. F. R.; Freitas, M. M. A.; Orfao, J. J. M. Modification of the surface chemistry of activated carbons. *Carbon* **1999**, *37*, 1379.

(26) Zielke, U.; Huttinger, K. J.; Hoffman, W. P. Surface-oxidized carbon fibers: I. Surface Structure and Chemistry. *Carbon* **1996**, *34*, 983.

(27) Puri, B. R. In *Chemistry and Physics of Carbon*; Marcel Dekker: New York, 1970.

(28) Bansal, R. C.; Donnet, J. B.; Stoeckli, F. *Active Carbon*; Marcel Dekker: New York, 1988.

(29) Marchon, B.; Carraza, J.; Heineman, H.; Somorjai, G. A. TPD and XPS Studies of O_2, CO_2 and H_2O Adsorption on Polycrystalline Graphite. *Carbon* **1988**, *26*, 570.

(30) Zhuang, Q.; Kyotani, T.; Tomita, A. DRIFT and TK/TPD Analyses of Surface Oxygen Complexes Formed during Carbon Gasification. *Energy Fuels* **1994**, *8*, 714.

(31) Zhuang, Q.; Kyotani, T.; Tomita, A. Dynamics of Surface Oxygen Complexes Drying Carbon Gasification with Oxygen. *Energy Fuels* **1995**, *9*, 630.

(32) Hall, P. J.; Calo, J. M.; Teng, H.; Suuberg, E. M.; May, J. A.; Lilly, W. D. The Nature of Carbon−Oxygen Complexes Produced by Different Oxidants: Towards a Unified Theory of Gasification? *Prepr. Pap. (Am. Chem. Soc., Div. Fuel Chem.)* **1989**, 112−121.

(33) Lizzio, A.; Radovic, L. R. Temperature-Programmed Desorption Studies of Coal Char Gasification. *Prepr. Pap. (Am. Chem. Soc., Div. Fuel Chem.)* **1989**, 102−111.

(34) Hall, P. J.; Calo, J. M. Secondary Interactions upon Thermal Desorption of Surface Oxides from Coal Chars. *Energy Fuels* **1989**, *3*, 370.

(35) Radovic, L. R.; Moreno-Castilla, C.; Rivera-Utrilla, J. Carbon Materials as Adsorbents in Aqueous Solutions. In *Chemistry and Physics of Carbon*; Radovic, L. R., Ed.; Marcel Dekker: New York, 2000; Vol. 27.

Received for review March 18, 2002
Revised manuscript received August 19, 2002
Accepted September 8, 2002

IE020210F